Journal of Power Sources 210 (2012) 7–14

Contents lists available at SciVerse ScienceDirect

Journal of Power Sources

journal homepage: www.elsevier.com/locate/jpowsour

Researches on current distribution and plate conductivity of valve-regulated lead-acid batteries

Tao Huang[a], Wenjun Ou[a], Bo Feng[a], Binbin Huang[a], Minyi Liu[a], Wenchao Zhao[b], Yonglang Guo[a,*]

[a] College of Chemistry and Chemical Engineering, Fuzhou University, Fuzhou 350108, PR China
[b] Chaowei Power Co. Ltd., Changxing, Zhejiang 313100, PR China

ARTICLE INFO

Article history:
Received 15 December 2011
Received in revised form 18 February 2012
Accepted 20 February 2012
Available online 2 March 2012

Keywords:
Active mass degradation
Conductivity
Current distribution
Ohmic polarization
Valve-regulated lead-acid batteries

ABSTRACT

A cell with tall plates was simulated by two cells and the controlled voltage with time was successfully used to measure the response current–time curves. It indicates that the current in the upper part of the plate is much higher than that in the lower part in early stage of the discharge, but in late stage, it is reversed, especially at high discharge rates. The upper part of the plate has higher capacity and deeper depth of discharge (DOD) so that the active mass degrades and sheds more quickly in cyclic applications. In the initial discharge, the lead sulfate formed at positive plates produces the internal stress and enhances the electric connection among the active mass particles. But the positive active mass only contributes a little to the conductivity of plates. The negative active mass with a bit shrinking but no passivation has better conductivity than the expanded active mass. The higher ohmic polarization of the active mass appears at higher discharge rates, in the upper part of the plates, in the late stage of the discharge, in aged battery, especially for negative plates.

1. Introduction

Grid corrosion, softening of the positive active mass and passivation of the negative active mass at high discharge rates are usually failure modes of flood and valve-regulated lead-acid (VRLA) batteries [1]. They are greatly affected by the current distribution on the plate surface, which is closely related to grid design and its conductivity, ohmic losses, the discharge rate [2,3]. All of these can be attributed to ohmic polarization on the plates.

The ohmic polarization on the plates in the vertical direction depends on the grid design and the conductivity of the entire plate. Consequently, a lot of work has been done on the grid design and computer simulation, to reduce ohmic loss and improve the current distribution. Sunu and Burrows [4–6] predicted the potential and current distributions on the surface of the orthogonal grids, according to each intersection and the conductivity of grid members. Morimoto et al. [7] used a finite difference method with a fine mesh to predict current density and potential distributions of the electrodes and the performance of any cell design using the measured voltage–current relationship of the active material. Tiedemann et al. [8] presented a model to calculate the potential distribution based on the assumption of a uniform current density. Calábek et al. [9–11] proposed that the configuration of current tabs played a considerable role in the utilization of the active material of plate accumulator electrodes during discharge, simulated current distribution of a positive–negative electrode pair and cylindrical VRLA cell, and optimized the orthogonal grid design. Ball et al. [12] investigated the effects of grid bar, its corrosion layer and grid shape on current density distribution and improved the grid design. Other simulation investigations including horizontal plates, spiral plates and micro-hybrid vehicle application have also been done [13–16]. In our previous works, an in situ electrochemical scan technique was established to study the current and potential distributions of various lead-acid battery plates based on the measurement of IR drop in the electrolyte between the positive and negative plates [17–21].

Softening and shedding of positive plates is a common failure mode in cyclic applications, especially in deep discharge, because the volumetric change from lead dioxide to lead sulfate causes mechanical stresses in the positive active mass [22]. Since there exists the ohmic loss in the vertical direction of the plates, the upper part of the plate has higher polarization, compared with the lower part. So at the beginning of discharge, the current density in the upper part of the plates, near the current collecting tab, is higher than that in the lower part. Consequently, the upper part has higher capacity, which is equivalent to deeper depth of discharge (DOD) [23–25].

Although a lot of work has been done on the current distribution investigations in terms of various simulations and models, it is difficult to measure the real current density in different parts

* Corresponding author. Tel.: +86 591 8807 3608; fax: +86 591 8807 3608.
E-mail address: yguo@fzu.edu.cn (Y. Guo).

0378-7753/$ – see front matter © 2012 Elsevier B.V. All rights reserved.
doi:10.1016/j.jpowsour.2012.02.086

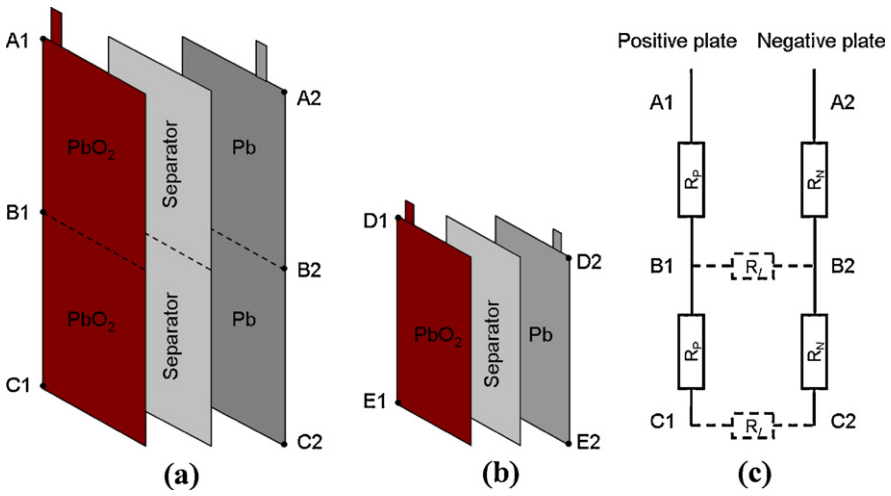

Fig. 1. The measurement scheme: (a) structure of 2 V 24 Ah cell simulated by two 2 V 12 Ah cells in parallel and their measurement points; (b) measurement points on positive and negative plates of 2 V 12 Ah cell; (c) equivalent circuit of two 2 V 12 Ah cells in parallel.

of the plates. The aim of this work is to establish a measurement method for the local current by controlling the voltage with time and to measure ohmic loss on the plates so as to gain an insight into the active mass degradation, battery failure mechanism and battery performance.

2. Experimental

The test batteries were 6-DZM-20 and 6-DZM-12 VRLA batteries used as electric bike, which were manufactured by Chaowei Power Co. Ltd., China. Each cell of the 6-DZM-20 VRLA battery was composed of four positive and five negative plates and the absorptive glass mat (AGM) separator. The 6-DZM-12 VRLA cell had seven positive and eight negative plates. The dimensions of positive grids of 6-DZM-20 and 6-DZM-12 VRLA batteries were 138 (H) × 66 (W) × 2.4 (T) and 72 (H) × 44.3 (W) × 2.4 (T) mm, respectively. The negative grids were heightened 1 mm because only positive plates were wrapped by AGM separators. The positive and negative grids with the lug at the corner and orthogonal design were cast by Pb–Ca–Sn–Al and Pb–Ca–Al alloys. The manufacture technologies and the designs of both batteries were the same. The apparent reaction areas of the positive plates for 6-DZM-20 and 6-DZM-12 VRLA batteries were 36.43 and 36.70 cm^2 Ah^{-1} and the C_2 capacities were 20 and 12 Ah, respectively.

To measure the current distribution and polarization of the plates, the positive and negative plates of a simulated 2 V 24 Ah VRLA cell were divided into two parts, i.e. the upper half and lower half in Fig. 1a. It is assumed that it had the same height as the plates of 2 V 20 Ah VRLA cell above, but the reaction area were enlarged proportionally. So two 2 V 12 Ah cells (Fig. 1b) were in parallel like Fig. 1a or c, but the current generated by the lower cell needed to flow through the plates of the upper cell, which led to the additional ohmic polarization of the upper half of the plate. In order to eliminate the voltage drop of the terminals, straps and lugs, the stainless steel screw were driven into A, B, C, D and E points in Fig. 1 through battery shell, respectively, to measure the ohmic losses of plates and battery voltages at different heights of plates.

The simulated 2 V 12 Ah cell was first discharged at constant current with 0.5, 1 and 3 C discharge rates with cut-off voltages of 1.75, 1.6 and 1.3 V, respectively. Then the corresponding voltage–time curve was used to control the discharge process of the simulated 2 V 12 Ah cell again, to obtain the response current with time and validate the measurement method.

The voltage–time curves used to control two simulated 2 V 12 Ah cells came from those recorded from points A_1A_2 and B_1B_2 at the corresponding discharge rates of 2 V 20 Ah cell, respectively. Since the discharge current of the cell is quite sensitive to the control voltage, it is important for each experiment to keep the same interval time after charging and the same start voltage before discharging. And the surrounding temperature of the test cell is controlled so as to make the cell have the same capacity. In order to avoid battery degradation, after the test batteries were discharged at high rates, they were normally cycled twice under the conditions of the 3.5 A 2.45 V current-limited constant voltage charge for 6–8 h and the discharge to 1.75 V cut-off voltage at 0.5 C rate. The experiments were conducted by Arbin BT2000 instrumentation and the data were acquired by HP34970A Data Acquisition/Switch Units.

To measure the resistance of positive and negative plates, the 6-DZM-20 VRLA battery with the same state of health (SOH) was torn down and the bottom of the wet plate was welded by a copper wire as collector. The active mass of positive plate was moved using a boiling solution containing 4 g of glucose and 20 g of sodium hydroxide in 200 g of distilled water, to get the entire grid [26]. The plate or grid resistance was calculated by measuring the voltage and current passing through the measured plate or grid. In the measurement of additional force, the pressure vertically forced onto the surface of the plate was recorded by the WTP204 load sensor.

3. Results and discussion

3.1. Measurement method of local current

One of the failure modes of lead-acid batteries for cyclic application, especially in the case of tall plates and deep discharge, is the softening of positive active mass located in the upper part of the plates or near the lug. It is attributed to the polarization in different regions, which leads to the uneven current distribution. In order to study the effects of the plate height and polarization on the current, Fig. 1c shows the equivalent circuit of two 2 V 12 Ah cells in parallel, in which only two electrolyte resistances instead of many resistances between positive and negative plates are used as a simple simulation, for the ohmic polarization in the vertical direction is the focus in this work.

The discharge curve of a battery is normally defined as the battery voltage–time curve obtained in the discharge at constant current. On the contrary, the responded current–time curve under

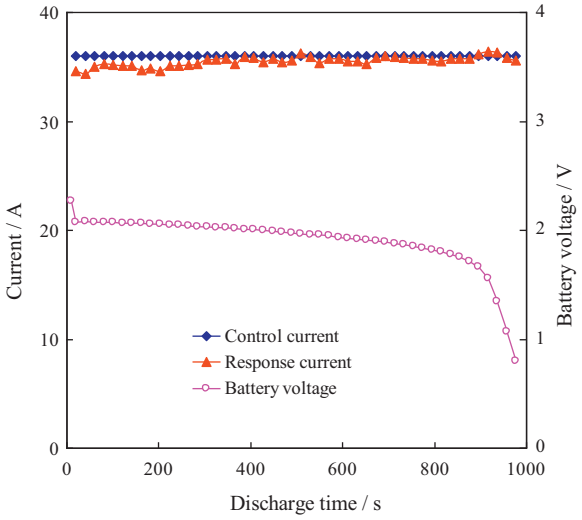

Fig. 2. The voltage–time curve of 2 V 12 Ah cell at 3 C discharge rate and the response current–time curve obtained when the voltage–time curve above was inversely used to control the 2 V 12 Ah cell.

the controlled voltage is seldom mentioned because it is very sensitive to the change of the control voltage. In the discharge at the controlled voltage, the cell voltages with time have 963 data at cut-off voltage of 0.8 V, but Fig. 2 shows only 1/20 points to make the curve clearer. It is found that the discharge current is relatively stable and the average current reaches 35.5 A which is very close to 3 C discharge rate. So the currents of two simulated 2 V 12 Ah cells in Fig. 1a or c can be measured by controlling the voltage with time which was obtained from the top (points A_1 and A_2) and the middle (points B_1 and B_2) of 2 V 20 Ah cell in the discharge of constant current, respectively.

Fig. 3 shows the change of the voltage with time between points A_1 and A_2 as well as B_1 and B_2 in Fig. 1 at 3 C discharge rate of 2 V 20 Ah cell. The voltage difference between two curves changes from about 26 to 29 mV, which is the sum of the voltage drop or ohmic polarization of the positive plate from points A_1 to B_1 and negative plate from points A_2 to B_2 in Fig. 1.

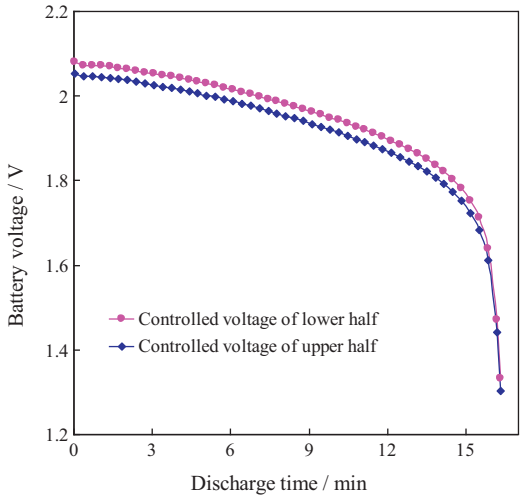

Fig. 3. The voltage–time curves used to control two 2 V 12 Ah cells which simulate the upper half and lower half of the tall cell at 3 C discharge rate.

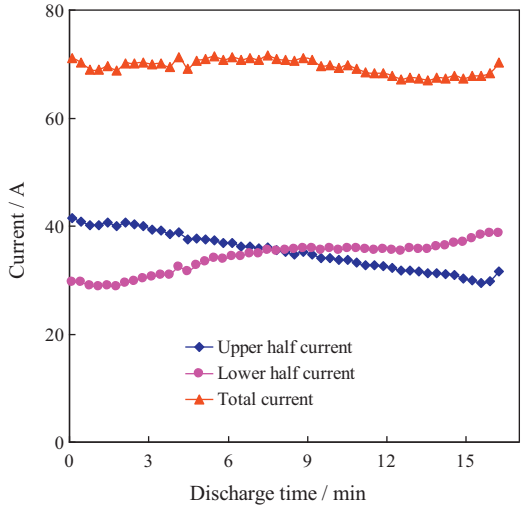

Fig. 4. The response current–time curves of the upper half, the lower half and entire cell at 3 C discharge rate.

3.2. Current distribution at different rates

The tall batteries like 2 V 20 Ah cells are usually applied to electric scooters. Their discharge rate is normally about 0.5 C but it can reach 1 C and higher in the acceleration. The higher discharge rates appear in the batteries of hybrid electric vehicle (HEV) applications. Figs. 4–6 show the changes in the current of the upper half and lower half of the simulated cell with time at 3, 1 and 0.5 C discharge rates, respectively. It can be seen that the total discharge current of the simulated 2 V 24 Ah cell are relatively stable and their corresponding average currents are 69.5, 23.3 and 12.2 A. The total current tends to be a little smaller at higher discharge rates. It may be attributed to greater concentration difference and larger electrolyte voltage drop.

It can be seen from Fig. 4 that the current in the upper half of the cell is obviously higher than that in the lower half from the beginning to the half-time of the discharge. The former decreases gradually while the latter increases with discharging. At the beginning of the discharge, the maximum current in the upper part reaches 41.5 A while it is only 29.5 A in the lower part. When the battery is discharged to 50% DOD at 3 C rate, the discharge capacities in the upper half and lower half are 5.13 and 4.26 Ah, corresponding

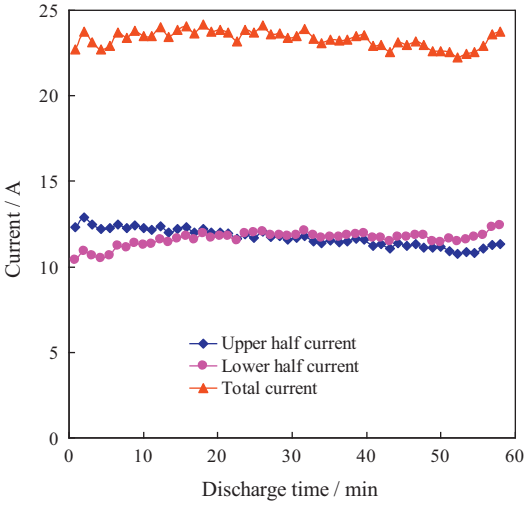

Fig. 5. The response current–time curves of the upper half, the lower half and entire cell at 1 C discharge rate.

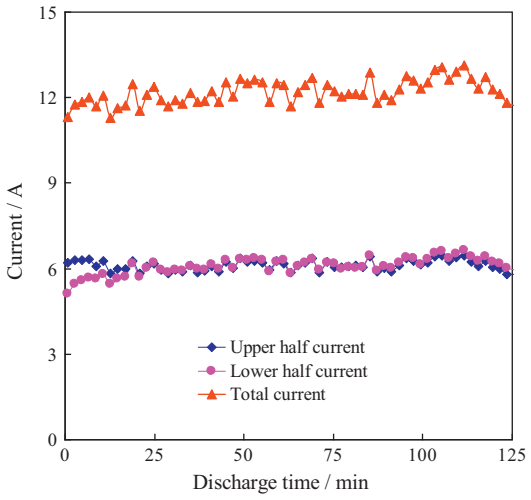

Fig. 6. The response current–time curves of the upper half, the lower half and entire cell at 0.5 C discharge rate.

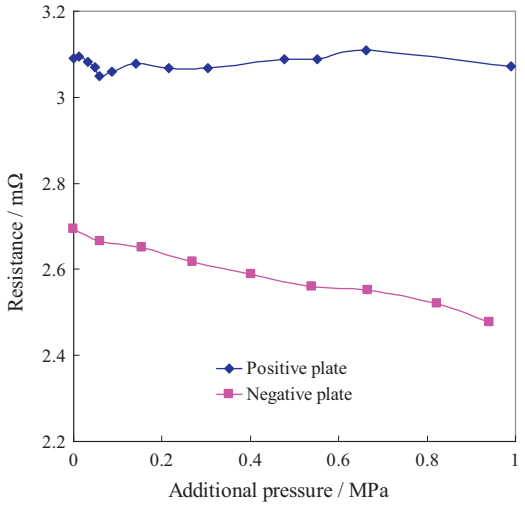

Fig. 7. The change of the resistance from bottom to top of wet positive and negative plates with additional pressure perpendicular to plate surface of a 6-DZM-20 VRLA battery.

to 54.5% and 45.3% DOD, respectively. The capacities and DOD in the upper half increase by 20% compared with those in the lower half. When the battery is continuously discharged to the cut-off voltage of 1.3 V cell^{-1}, i.e. 100% DOD, their capacities are 9.63 and 9.30 Ah and the capacity in the upper half is 1.04 times of that in the lower half.

As the discharge current or discharge rate decreases, the tendencies of the current change in Figs. 5 and 6 are similar, but the difference between upper and lower parts become smaller and smaller. In the initial 6 min discharge, the average currents in the upper half and lower half are 12.43 and 10.72 A at 1 C rate, 6.28 and 5.45 A at 0.5 C rate, respectively. The 100% DOD capacities in the upper half and lower half are 11.52 and 11.41 Ah at 1 C rate, 12.99 and 12.92 Ah at 0.5 C rate. Therefore, the higher the discharge current is, the greater the difference between the upper and lower parts becomes.

In the discharge of the battery, there exist various polarizations including charge transfer, η_{ct}, concentration difference, η_c, electrolyte resistance, η_{sol}, connect resistance among active mass particles in horizontal direction, η_{AM}, and plate resistance in the vertical direction, η_p. If E_{oc} defines the voltage on open circuit, the battery operating voltage at the top of the plate, E^H, is equal to

$$E^H = E_{oc} - (\eta_{ct}^H + \eta_c^H + \eta_{sol}^H) - \eta_{AM}^H \quad (1)$$

where H is the total height of the plate. When the current passes from the positive plate to negative plates at the given height of the plate, h, the battery operating voltage can also be expressed by

$$E^H = E_{oc} - (\eta_{ct}^h + \eta_c^h + \eta_{sol}^h) - \eta_{AM}^h - \eta_p^h \quad (2)$$

Therefore, the polarization in parentheses above $(\eta_{ct}^h + \eta_c^h + \eta_{sol}^h)$, decreases with the increase of the ohmic polarization, η_p^h, caused by the current passing from bottom to the given height of the plate when the active mass has not been passivated, i.e. when η_{AM} is small. The lower the given height on the plate is, the smaller the polarizations of $(\eta_{ct}^h + \eta_c^h + \eta_{sol}^h)$ in the lower part of the plate are and then the lower the local current density in this region becomes. The difference of the discharge current and DOD between the top and bottom is the greatest. In practice, the battery discharge is normally less than 100% DOD or very shallow like the automobile batteries or it has very high discharge rates like HEV batteries. All this can make the active mass located at the top of the plates discharge frequently and deeply, which promotes the softening of positive active mass near grid tabs and in the upper part.

3.3. Resistance of plates and grid

One of the failure modes of lead-acid batteries for various applications is the corrosion of positive grid which is a current collector besides being a supporter of active mass. In order to know the contribution of grids and active mass to the conductivity, the resistances of the individual grid and the charged plate with sulfuric acid electrolyte, torn from new and used 6-DZM-20 VRLA batteries, were measured and shown in Table 1. It indicates that the resistance of the positive grid is smaller than that of negative grid because the former is thicker and heavier. For the new battery, the resistance of the positive plate with the electrolyte only decreases a little compared with its grid resistance, but great changes occur at negative plate. The positive and negative grids have 89% and 61% of the conductivity of their corresponding plates. For the used but healthy battery with 165 charge–discharge cycles, the resistance of the positive grid becomes high because of its corrosion. It is interesting to note that the resistance of the negative plate is much smaller than that of its grid. The positive and negative grids have 91% and 49% of the conductivity of their corresponding plates. This is because the negative active mass is built of the skeleton network

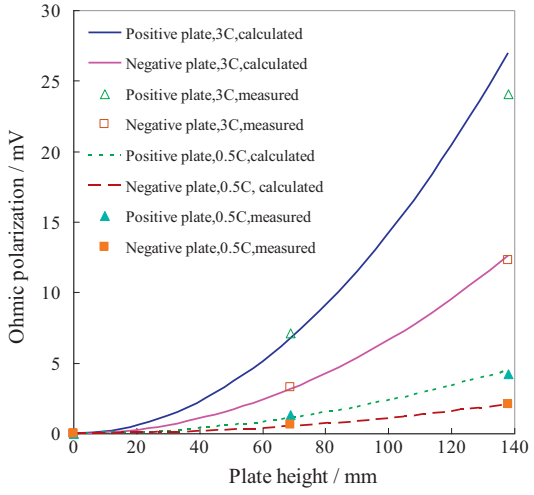

Fig. 8. The dependence of the calculated and measured ohmic polarization of the positive and negative plates on the height at 3 and 0.5 C discharge rates.

Table 1
The resistance of individual plate with electrolyte and individual grid of 6-DZM-20 VRLA battery.

Samples	Positive grids (mΩ)	Positive plates (mΩ)	Negative grids (mΩ)	Negative plates (mΩ)
New battery	3.71	3.30	4.41	2.69
Used battery	3.96	3.60	4.29	2.10

as current conductor and energetic structure composed of small crystals which participate in the charge and discharge processes. With cycling, the expander disintegrates and part of lead particles from the energetic structure is deposited onto the skeleton to make the negative active mass shrink and its conductivity become high [27,28]. Therefore, the constrictive and compact active mass of the negative plate without passivation has better conductivity compared with the expanded sponge lead.

In the discharge of the battery, both the reduction of PbO_2 to $PbSO_4$ and the oxidation of Pb to $PbSO_4$ make their active masses expand and produce the internal stress. In order to understand the effects of the compression on the conductivity, Fig. 7 shows the resistance changes of the wet positive and negative plates with sulfuric acid electrolyte with the additional pressure perpendicular to plate surface. It is found that the resistance of the negative plate decreases with the additional pressure. This is in agreement with the results above. It is the same case with the positive plate but only at a low pressure. When the pressure exceeds 60 kPa, the conductivity of the positive active mass inversely becomes poor. This may be due to the difference between the force perpendicular to plate surface and the internal stress of active mass. The former has only one direction and easily destroys the structure of positive active mass. While the volume of the latter increases, the PbO_2 particles are squeezed and the electrical connection will be improved.

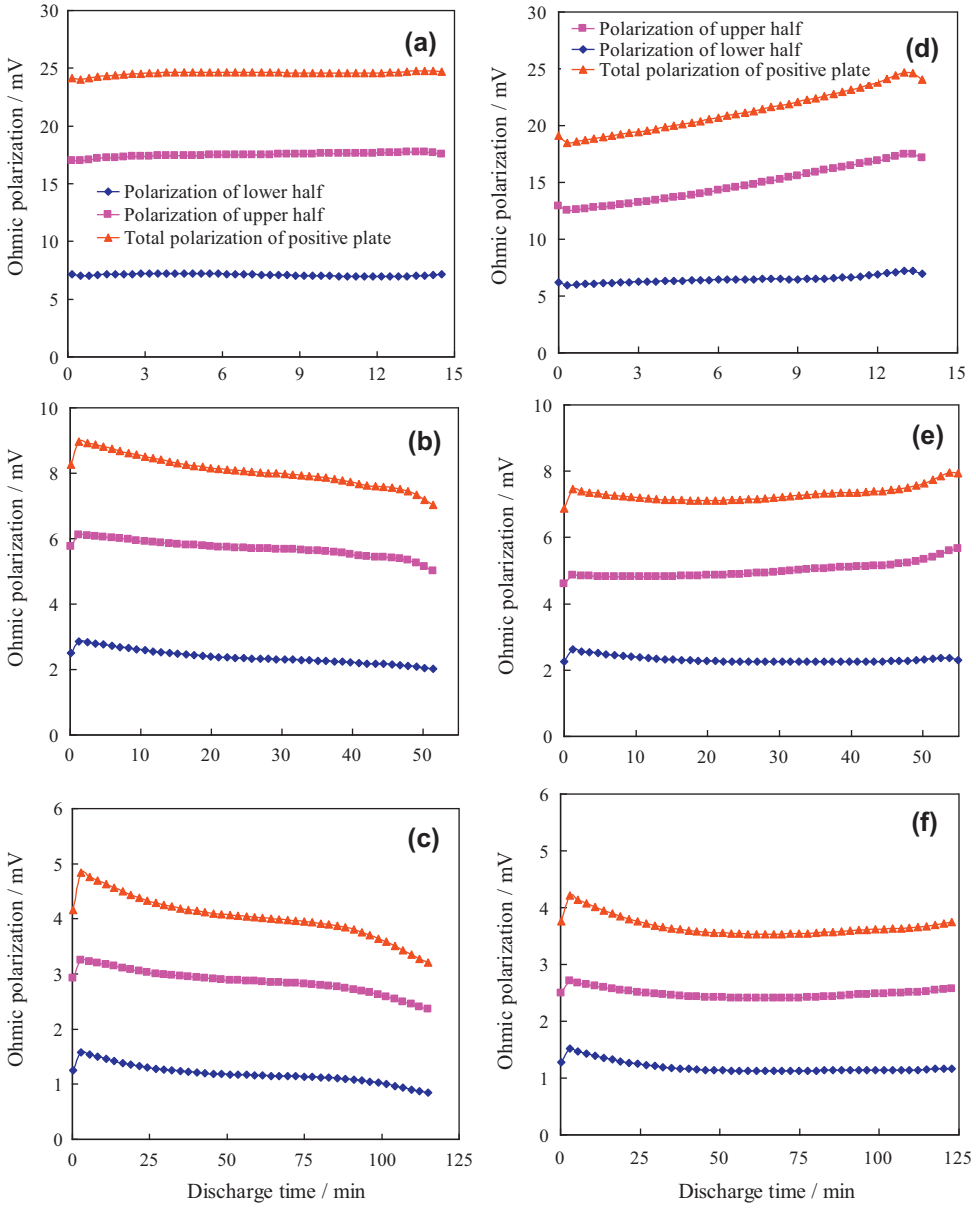

Fig. 9. The evolution of the ohmic polarization of the upper half, the lower half and the entire positive plate of the used (left) and new (right) 2 V 20 Ah cell. Discharge rates: (a), (d) 3 C; (b), (e) 1 C; (c), (f) 0.5 C.

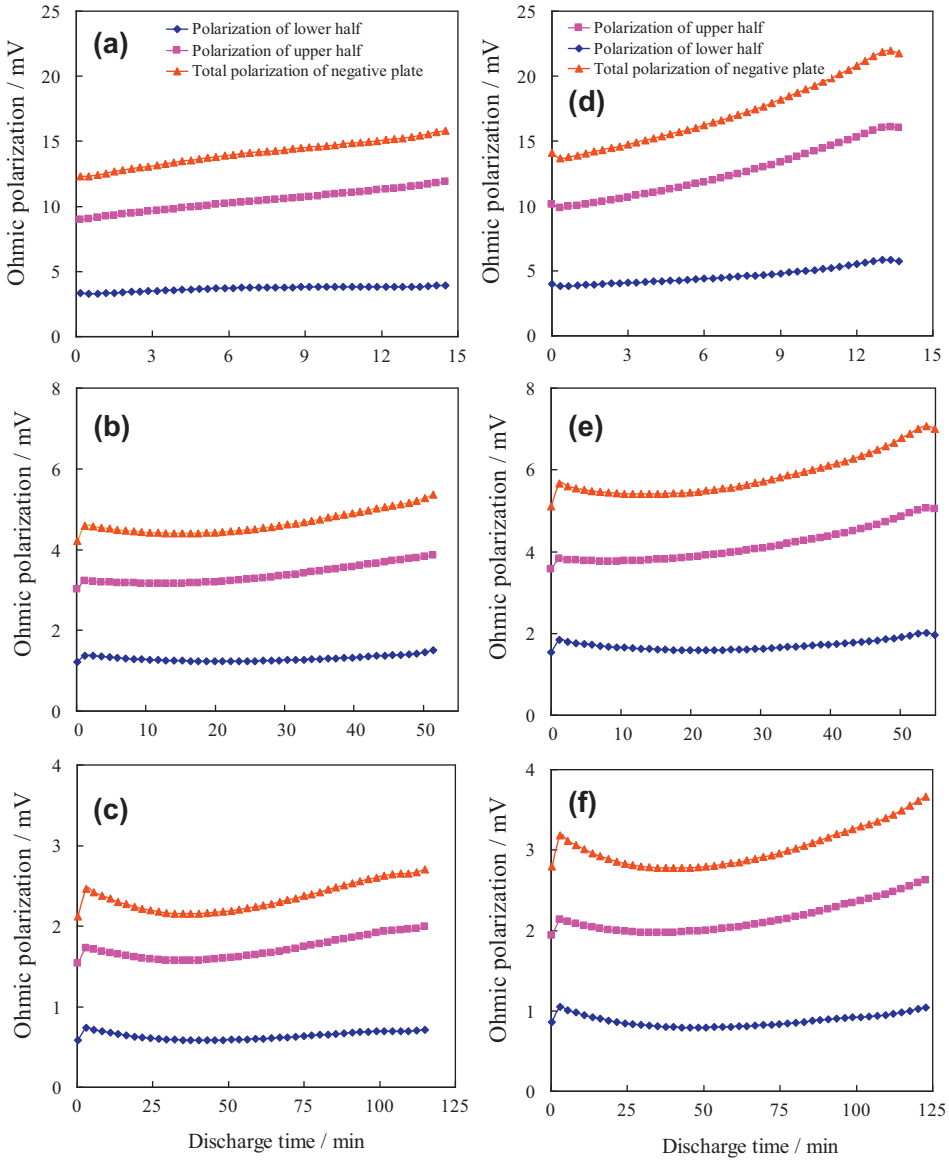

Fig. 10. The evolution of the ohmic polarization of the upper half, the lower half and the entire negative plate of the used (left) and new (right) 2 V 20 Ah cell. Discharge rates: (a), (d) 3 C; (b), (e) 1 C; (c), (f) 0.5 C.

3.4. Ohmic polarization on plates

When the current produced on the plate passes to the lug in the charge–discharge, the ohmic polarization of the plate in the vertical direction varies greatly with the height of the plate. If the generated current density, i, is the same on the plate, the current, I_h, passing through the given height of the plate, h, is

$$I_h = iWh \tag{3}$$

where W is the width of the plate. If H and R_H denote the total height and the resistance from bottom to top of the plate, respectively, the resistance from bottom to the given height of the plate, R_h, is.

$$R_h = \frac{R_H}{H} \cdot h \tag{4}$$

Therefore, the ohmic polarization from bottom to the given height of the plate, η_p, and its change rate with height can be expressed by, respectively

$$\eta_p = \int_0^h iWh \cdot \frac{R_H}{H}\, dh = \frac{1}{2} I R_H \frac{h^2}{H^2} \tag{5}$$

$$\frac{d\eta_p}{dh} = \frac{IR_H}{H^2} h \tag{6}$$

By the calculation based on Eq. (5) above and the experiment measurements, Fig. 8 shows the dependence of the ohmic polarization of the positive and negative plates in the vertical direction on the given height at 0.5 and 3 C discharge rates. The experiment values are well in agreement with the results in Eq. (5). Only at the top where the current reaches maximum are the experiment values a little smaller. When $h = 0.5H$, $\eta_p^h = 0.25\eta_p^H$. That is to say, the ohmic polarization in the lower half is only a quarter of that of whole plate and the maximum polarization appears at the top of

the plate due to the current passing from bottom to top of the plate and collecting to the lug.

In order to further understand the ohmic polarization at different heights of the plates, Figs. 9 and 10 show the change in the ohmic polarization of the upper half, the lower half and the entire positive and negative plates when the new and used but healthy batteries were discharged at 3, 1 and 0.5 C rates, respectively. The "used" battery has been charged and discharged 165 cycles at 0.5 C discharge rate. Its state of health (SOH) is in the middle for the battery life of 300–350 cycles. All experiment data in Figs. 9 and 10 indicate that the ohmic polarization of the upper half of the positive and negative plates is much higher than that of their lower half.

For the used battery, the ohmic polarization of the upper half and the lower half of the positive plate almost remains unchanged at 3 C discharge rate in Fig. 9a, but it decreases gradually with discharging at 1 and 0.5 C discharge rates in Fig. 9b and c. This is because a lot of tiny $PbSO_4$ particles with insulator are formed at 3 C discharge rate, which does not contribute to the conductivity. At low discharge rate in Fig. 9b and c, however, larger and more $PbSO_4$ particles are produced, which results in larger volume expansion and the internal stress in positive active mass. Based on the aggregate-of-spheres model (AOS) [25,29], the conductivity of the positive active mass depends on the interconnection and area of the "bottle-neck" between the individual particles. The volume expansion and internal stress in active mass enhance the contact of PbO_2 particles and then improve their electric connection. Therefore, the conductivity of the positive active mass increases gradually and the ohmic polarization decreases slowly at low discharge rates.

For the positive plate of the new battery in Fig. 9d–f, the ohmic polarizations are obviously smaller compared with the used battery in Fig. 9a–c, indicating that the grid corrosion and slight active mass degradation occur at the positive plate of the latter, which reduces the conductivity of the plates. At 3 C discharge rate in Fig. 9d, the ohmic polarization of the positive plate increases continuously to the value at the end of the discharge, which is closed to the ohmic polarization of the used battery in Fig. 9a. At 1 and 0.5 C discharge rates in Fig. 9e and f, the ohmic polarizations of the positive plate decreases a little and then also increases slightly with discharging. It becomes more obvious with the decrease of the discharge rate. It is also found that the ohmic polarizations of positive plates at the end of the discharge for the new and used batteries tend to be almost the same value at the corresponding discharge rate. It reveals that the positive active mass expands in the initial discharge, which is helpful to the conductivity of positive plates. And then more lead sulfates with insulator are formed with continuous discharging and the resistance in the positive active mass increases. Although the volume expansion and internal stress in positive active mass can enhance the conductivity of active mass, the active mass contributes only a little to the conductivity of positive plates for both new and used batteries.

In the case of the negative plates in Fig. 10, their ohmic polarizations are much smaller than those of the positive plates in Fig. 9. And it is interesting to note that the ohmic polarizations of the negative plates for the used battery in Fig. 10a–c are much lower than those for the new battery in Fig. 10d–f. It is clear that the negative active mass makes a great contribution to the conductivity of the negative plate. After the battery is used for a period, some expanders in the negative active mass is decomposed partly, which makes the negative active mass shrink slightly and a little compact structure formed. The negative active mass with compact structure and coarse skeleton has better conductivity than that with expanded structure [27,28].

At 3 C discharge rate in Fig. 10a and d, the ohmic polarizations of the negative active mass become increasingly high with discharging. In the initial discharge at 1 and 0.5 C rates in Fig. 10b, c and e, f, however, they drop a little and then increase slowly. And it becomes more obvious with the decrease of the discharge rate. This is attributed to interaction of two factors: conductor of the sponge lead and insulator of lead sulfate. At low discharge rates, the formed lead sulfate crystals are large and do not passivate the negative active mass obviously, but they can produce the internal stress in the negative active mass, which can enhance the conductivity of the sponge lead. As the negative plates are discharged continuously, more lead is transformed into lead sulfates with insulator. The contribution of the active mass to the conductivity becomes increasingly small. At high discharge rate in Fig. 10a and d, the negative active mass is passivated by the fine lead sulfate crystals with compact structure, which reduces the conductivity. And in this case, the ohmic polarization caused by the fine lead sulfate crystals becomes dominant.

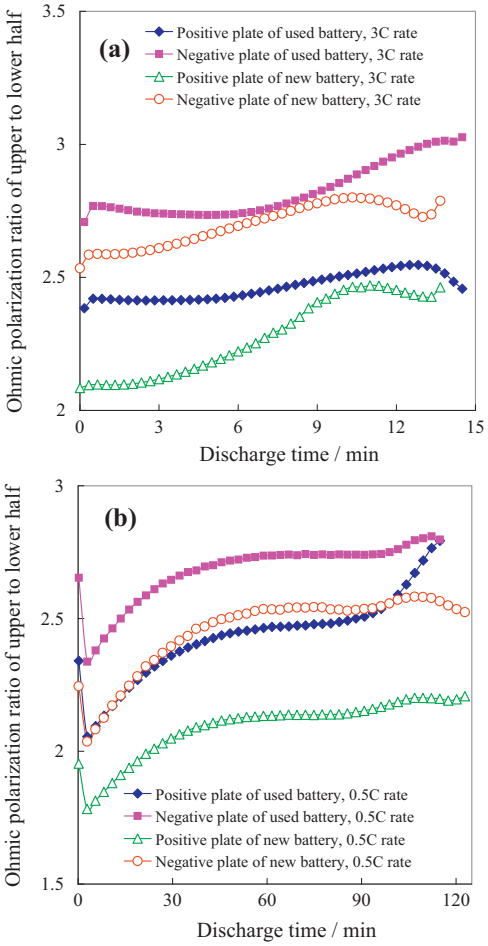

Fig. 11. The ohmic polarization ratio of upper half to lower half of positive and negative plates for the used and new batteries. Discharge rates: (a) 3 C; (b) 0.5 C.

3.5. Evolution of active mass resistance in different parts of plates

Since the positive and negative active masses also contribute to the conductivity besides grids, their degradation and part passivation caused by different current distributions and different DOD can result in the increase of the active mass resistance or ohmic polarization. Fig. 11 shows the ohmic polarization ratios of upper to lower half of positive and negative plates for the used and new 2 V 20 Ah cells, respectively. The larger ratio indicates the higher resistance of active mass in the upper part and the nonuniformity on the plate. It is found that more unevenness appears on the negative plates of both used and new batteries, although the negative

plate has better conductivity shown in Table 1, compared with the positive plate. In comparison with 0.5 C discharge rate in Fig. 11b, the resistance of active mass in the upper part increases obviously at 3 C discharge rate in Fig. 11a. And it becomes increasingly high in the discharge for both positive and negative plates of the used and new batteries at different discharge rates. Furthermore, the resistance in the upper part of the used battery is higher than that of the new battery, indicating that more obvious degradation of active mass occurs in the upper part of both positive and negative plates of the used battery. Therefore, higher resistance appears in the upper part of the plates, at higher discharge rate and at the end of the discharge, which accelerates the active mass degradation, especially for the negative plate. So the copper-stretch-metal (CSM) grid with coating lead is often used for the negative grid of large batteries to reduce the ohmic polarization of the negative plates and greatly improves the current distribution and then the performance of the batteries.

4. Conclusions

To understand the current distribution and the uniformity on the plates of tall batteries, the upper and lower parts of a tall cell were simulated by two cells and the response current with time was successfully measured by controlling the voltage changes with time. Since the current passing along the plates can lead to the ohmic loss of the plates, its upper part has higher polarizations of charge transfer, concentration difference and electrolyte, compared with its lower part. At the beginning of 3 C discharge rate, the currents in upper half and lower half of the simulated cell reaches 41.5 and 29.5 A, respectively. The upper part of the plate has higher capacity and deeper DOD, especially at high discharge rates.

The positive active mass only contributes a little to the conductivity of plates. In the discharge, the lead sulfate particles formed at positive plates can produce the internal stress and enhance the electric connection among the active mass particles, which is helpful to the conductivity of the positive plate. The negative active mass which shrinks a little in the used battery has better conductivity than the expanded active mass of the new battery. At high discharge rates, however, the passivation of the fine and compact lead sulfate product becomes dominant.

The highest ohmic polarization of the plates occurs at the top of the plate. The ohmic polarization in the lower half of the plate is only about a quarter of that of the whole plate. The higher ohmic polarization of the active mass appears at higher discharge rate, in the upper part of the plate, in the late stage of the discharge, in aged battery, especially for the negative plate. All this will accelerate the degradation of the active mass.

Acknowledgement

The authors are grateful to NSFC (No. 51072037) in China for financial support for this work.

References

[1] P. Lailler, F. Zaninotto, S. Nivet, L. Torcheux, J.-F. Sarrau, J.-P. Vaurijoux, D. Devilliers, J. Power Sources 78 (1999) 204–213.
[2] N.E. Bagshaw, K.P. Bromelow, J. Eaton, in: D.H. Collins (Ed.), Power Sources, vol. 6, Academic Press, New York, 1977, p. 1.
[3] G. Maia, E.A. Ticianelli, E.R. Gonzalez, J. Appl. Electrochem. 23 (1993) 1151–1161.
[4] W.G. Sunu, B.W. Burrows, J. Electrochem. Soc. 128 (1981) 1405–1411.
[5] W.G. Sunu, B.W. Burrows, J. Electrochem. Soc. 129 (1982) 688–695.
[6] W.G. Sunu, B.W. Burrows, J. Electrochem. Soc. 131 (1984) 1–6.
[7] Y. Morimoto, Y. Ohya, K. Abe, T. Yoshida, H. Moromoto, J. Electrochem. Soc. 135 (1988) 293–298.
[8] W. Tiedemann, J. Newman, F. DeSua, in: D.H. Collins (Ed.), Power Sources, vol. 6, Academic Press, New York, 1977, p. 15.
[9] M. Calábek, K. Micka, P. Bača, P. Křivák, J. Power Sources 85 (2000) 145–148.
[10] P. Křivák, P. Bača, M. Calábek, K. Micka, P. Král, J. Power Sources 154 (2006) 518–522.
[11] P. Král, P. Křivák, P. Bača, M. Calábek, K. Micka, J. Power Sources 105 (2002) 35–44.
[12] R.J. Ball, R. Evans, R. Stevens, J. Power Sources 103 (2002) 213–222.
[13] J. Kowal, D. Schulte, D.U. Sauer, E. Karden, J. Power Sources 191 (2009) 42–50.
[14] K. Yamada, K. Maeda, K. Sasaki, T. Hirasawa, J. Power Sources 144 (2005) 352–357.
[15] Z. Mao, R.E. White, B. Jay, J. Electrochem. Soc. 138 (1991) 1615–1620.
[16] J.N. Harb, R.M. LaFollette, J. Electrochem. Soc. 146 (1999) 809–818.
[17] Y. Guo, W. Li, L. Zhao, J. Power Sources 116 (2003) 193–202.
[18] Y. Guo, Y. Li, G. Zhang, H. Zhang, J. Garche, J. Power Sources 124 (2003) 271–277.
[19] Y. Guo, T. Wu, M. Zhang, J. Electrochem. Soc. 152 (2005) A415–A420.
[20] Y. Guo, X. Zhou, M. Huang, H. Liu, J. Power Sources 157 (2006) 571–578.
[21] Y. Guo, H. Liu, J. Power Sources 183 (2008) 381–387.
[22] J. Yan, W. Li, Q. Zhan, J. Power Sources 133 (2004) 135–140.
[23] P.E. Baikie, M.I. Gillibrand, K. Peters, Electrochim. Acta 17 (1972) 839–844.
[24] Y. Guo, S. Tang, G. Meng, S. Yang, J. Power Sources 191 (2009) 127–133.
[25] E. Meissner, J. Power Sources 78 (1999) 99–114.
[26] W.X. Guo, D. Shu, H.Y. Chena, A.J. Li, H. Wang, G.M. Xiao, C.L. Dou, S.G. Peng, W.W. Wei, W. Zhang, H.W. Zhou, S. Chen, J. Alloy Compd. 475 (2009) 102–109.
[27] D. Pavlov, V. Iliev, J. Power Sources 7 (1981) 153–164.
[28] V. Iliev, D. Pavlov, J. Appl. Electrochem. 15 (1985) 39–52.
[29] A. Winsel, E. Voss, U. Hullmeine, J. Power Sources 30 (1990) 209–226.